Available online at www.sciencedirect.com
SCIENCE DIRECT®
Carbohydrate Research 338 (2003) 977–986
CARBOHYDRATE RESEARCH
www.elsevier.com/locate/carres

X-ray structure of the cyclomaltohexaicosaose triiodide inclusion complex provides a model for amylose–iodine at atomic resolution

O. Nimz,[a,1] K. Geßler,[a,2] I. Usón,[b] S. Laettig,[c] H. Welfle,[c] G.M. Sheldrick,[b] W. Saenger[a,*]

[a]*Institut für Kristallographie, Freie Universität Berlin, Takustrasse 6, D-14195 Berlin, Germany*
[b]*Institut für Anorganische Chemie, Universität Göttingen, Tammannstrasse 4, D-37077 Göttingen, Germany*
[c]*Max-Delbrück-Centrum für Molekulare Medizin, Robert-Rössle-Str. 10, D-13092 Berlin-Buch, Germany*

Received 15 August 2002; received in revised form 16 December 2002; accepted 6 January 2003

Abstract

Cyclomaltohexaicosaose (CA26) is folded into two $1^2/_3$ turns long V-helices that are oriented antiparallel. Crystals of complexes of CA26 with NH_4I_3 and $Ba(I_3)_2$ are brown and X-ray analyses show that I_3^- units are located in the ~ 5 Å wide central channels of the V-helices. In the complex with NH_4I_3, two CA26 molecules are stacked to form $2 \times 1^2/_3$ turns long channels harbouring 3 I_3^- at 3.66–3.85 Å inter I_3^- distance (shorter than van der Waals distance, 4.3 Å), whereas in the $Ba(I_3)_2$ complex, CA26 are not stacked and only one I_3^- each fills the V-helices. Glucose···I contacts are formed with C5–H, C3–H, C6–H and (at the ends of the V-helices) with O6 in (+) *gauche* orientation. By contrast, O2, O3, O4 and O6 in the preferred (−) *gauche* orientation do not interact with I because these distances are ≥ 4.01 Å and exceed the van der Waals I···O sum of radii by about 0.5 Å except for one O2···I distance of 3.68 Å near the end of one V-helix. Raman spectra indicate that the complexes share the presence of I_3^- with blue amylose–iodine.

Keywords: Amylose–iodine; Cyclomaltohexaicosaose triiodide inclusion complexes; Triiodide inclusion complex; CA26; X-ray structures

1. Introduction

The dark blue complex formed between iodine and amylose (that consists of a chain of α-(1→4) linked glucose units) is known since 1814,[1] but details of its structure and the nature of the iodine are still under discussion.[2–4] The gross structure of the amylose–iodine complex was first determined by X-ray fiber-diffraction[5,6] and described as folding of amylose into a V-helix with left-handed screw sense, six glucoses per turn and 8 Å pitch. In the central, ~ 5 Å wide channel-like cavity of the V-amylose helix, polyiodide is embedded with average I···I distance of 2.9 Å. The exact form of this polyiodide has since then been disputed and studied by Resonance Raman and circular dichroism,[3,7–9] absorption,[3,4] Mössbauer[10] spectroscopy, calorimetry,[11] iodine L-edge X-ray absorption fine structure (XAFS),[12] other physical methods[2] and theory.[3,4,11,13,14] The data have been interpreted as a linear chain of equidistant iodine atoms,[8] I_2 and larger associates,[2,11] triiodide (I_3^-), pentaiodide (I_5^-) and higher iodides[2–4,6,7,10,12] or a mixture of these species according to an equilibrium model assuming coexistence of I_3^- and I_5^- substructures in the amylose–iodide complex whose balance depends on experimental conditions.[3] Crystallization of well-defined fragments of amylose with iodine/iodide remained elusive except for *p*-nitrophenylmaltohexaose that crystallized in the form of a left-handed, antiparallel double helix with $(I_3^-)_n$ located in the central channel.[15] Several model compounds were used to simulate the amylose–iodine complex,[7–10] the closest being α-cyclodextrin as it resembles in its dimensions and chemical nature one turn of V-amylose. In complex with polyiodide, α-cyclodextrin forms a chan-

* Corresponding author. Tel.: +30-838-3412; fax: +30-838-6702
E-mail address: saenger@chemie.fu-berlin.de (W. Saenger).
[1] Present address: CallistoGen AG, Neuendorf Str. 24b, D-16761 Germany.
[2] Present address: Xerox GmbH, Vor dem Lauch 15, D-70567 Stuttgart, Germany.

0008-6215/03/$ - see front matter
doi:10.1016/S0008-6215(03)00016-8

nel-type structure, the channel being occupied by disordered $(I_2I_3^-)_n$ or $(I_5^-)_n$, depending on counterion Li^+ and Cd^{2+}, respectively.[16]

Recently, very large cycloamyloses ranging from 10 to 32 glucoses in the macrocycle were prepared.[17,18] The crystal structure of the hydrated cyclomaltohexaicosaose (CA26) shows that the macrocycle is folded like the figure '8', with almost two ($1^2/_3$) turns long V-amylose helices in antiparallel orientation related by a pseudo-C_2 axis.[19,20] The complex formation between I_3^- and CA26 analogs with 21–32 glucoses (DP21 to DP32) was investigated with isothermal titration calorimetry (ITC).[21] The data suggest that CA26 has two identical binding sites, each occupied by one I_3^-, in agreement with the folding structure of CA26. In the present contribution, we report the structure of CA26 crystallized as I_3^- inclusion complex with NH_4^+ and Ba^{2+} as counterions that shows atomic details of amylose···I interactions and provides a new model for amylose–iodine.

Table 1
Crystallographic data

	I	II
Chemical formula	$2(C_{156}H_{260}O_{130})\cdot 6NH_4I_3\cdot 2NH_4I\cdot 91.5H_2O$	$(C_{156}H_{260}O_{130})_{0.5}\cdot Ba_{0.5}I_3\cdot 23.75\cdot H_2O\cdot (PEG400)_{0.5}$·glycol
Formula weight	12761.0	3113.2
Space group	$C222_1$	$C2$
Temperature (K)	100	300
Wavelength (Å)	0.92	0.75
Unit cell constants		
a (Å)	31.79(3)	50.70(1)
b (Å)	44.13(4)	13.853(3)
c (Å)	80.65(8)	21.429(4)
α (°)	90	90
β (°)	90	114.57(3)
γ (°)	90	90
Volume (Å^3)	113,143	13,687
Crystal size (mm)	$0.5\times0.3\times0.1$	$0.3\times0.2\times0.1$
Calculated density (g/cm^3)	1.35	1.46
Resolution range (Å)	10.0–0.91	23.0–0.90
Measured reflections	182,685	45,274
Unique reflections: all data	32,818	8824
with $\geq 4\sigma$ (F_{obs})	31,978	7880
Completeness (%)	92.0	98.6
R_{sym} (%)	9.8	4.3
Parameters	6451	1685
Final R-factor: all data	0.085	0.087
with $\geq 4\sigma$ (F_{obs})	0.084	0.080
R_{Free}: all data	0.101	0.102
with $\geq 4\sigma$ (F_{obs})	0.100	0.092
Goodness-of-fit	1.973	1.877
$\Delta(\rho)_{max}$, $\Delta(\rho)_{min}$ [e/Å^3]	0.99, −0.87	0.56, −0.45

2. Experimental

Preparation and purification of CA26 are as previously described.[17–19] Complexes of CA26 and polyiodide were prepared by mixing 3 μL of 20 mg CA26/mL H_2O, 1 μL saturated aqueous NH_4I_3 or $Ba(I_3)_2$, respectively and 3 μL aqueous 25% (vol/vol) polyethyleneglycol (PEG400). The drops were equilibrated against a PEG400/H_2O reservoir (25% vol/vol, 10 mL) according to the hanging drop vapour diffusion method. After several days, brown prismatic crystals formed with characteristics given in Table 1. In the following, the complex with NH_4^+ counterions is designated (**I**) and the one with Ba^{2+} counterions (**II**).

X-ray diffraction data to 0.9 Å resolution were measured at beamline X31 (EMBL outstation at DESY/Hamburg) at 100 (**I**) and 300 K (**II**); using wavelengths given in Table 1. Data of crystals **II** could not be measured at lower temperatures because all attempts to establish conditions for shock-freezing the crystals remained elusive. The data were processed with the HKL program suite,[22] and symmetry equivalent reflections were merged to yield the final data set described in Table 1.

Attempts to solve the phase problem by molecular replacement using CA26[19] as search model failed due to the strong contribution of I_3^- (that is partially disordered) to the structure amplitudes. The crystal structure of **I** was finally determined by dual-space recycling methods as implemented in the program SHELXD[23] using data to a resolution of 1.05 Å. The internal loop, which operates only on the strongest E magnitudes (in this case, 3559 $E > 1.4$) was set to locate the 18 highest occupied iodine sites. Starting from a trial set of randomly positioned atoms consistent with the Patterson function, phases were refined by the tangent formula[24] in reciprocal space, alternating with the selection of the 30 highest peaks in an E-map. Twelve of these potential atoms were then eliminated at random. After 10 such real/reciprocal space iteration cycles, possible solutions for **I** were screened by checking the value of the correlation coefficient (CC) based on all data[25] and the value of the Patterson superposition minimum function for the highest occupied 18 iodine (6 I_3^- sites) and 2 iodide (I^-) sites (PATFOM). Partial solutions with a CC above 40% and PATFOM above 15 invariably led to a structure determination characterized by a CC of almost 70% when expanded by eight cycles of progressive

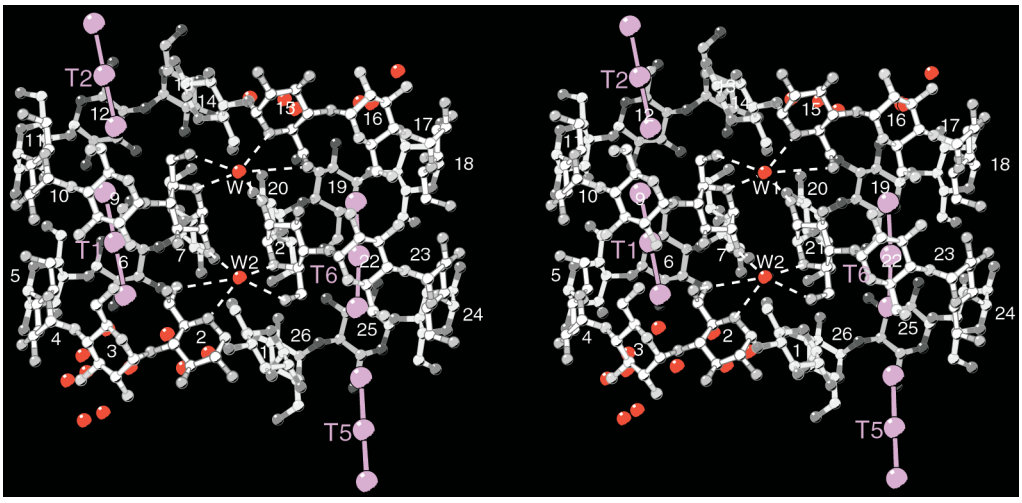

Fig. 1. Stereo view of complex **I**, CA26 in white/grey with glucoses numbered 1–26. Some of the water molecules in **I** shown in red, with the structurally important water W1 and W2 labeled. The pseudo-twofold rotation axis relating the two halves of CA26, glucoses G1–G13 and G14–G26, is perpendicular to the paper plane and located between W1 and W2. The triiodides T1, T2 and T5, T6 shown in magenta, T3 and T4 not shown as they bind to adjacent CA26 molecules which participate in the formation of the symmetry-independent V-helix channels, see Fig. 4.

incorporation of more atoms and peaklist optimisation[26] from bottom to top. During this process, atoms were eliminated whenever this led to an improvement of the CC between observed and calculated normalized structure factors based on all data. After 100 random trials, the structure was solved in three approaches, each leading to the location of 740 atoms in nearly identical sites. The number of iodine atoms to be located in the internal loop proved to be a critical parameter that had to be determined before arriving at an undistorted, fairly complete solution. It was optimized by examining the values of the Patterson function relating possible iodine atom pairs and led to the determination of all major iodine sites in the structure.

The location of the barium ion in **II** at 0.5, 0.5, 0.5 could be determined from the Patterson function after statistically removing the origin peak. Expansion of this one-atom partial solution by five cycles of progressive incorporation of more atoms and peaklist optimisation based on all data as explained above led to the determination of the whole structure, characterized by a CC of 76% and location of 139 correct atom sites.

Both crystal structures were refined by full-matrix least-squares with SHELXL97,[27] restraining glucose and triiodide 1–2 and 1–3 interatomic distances. Difference electron densities provided the positions of the remaining atoms of the structure (disordered I positions, disordered water and CA26 primary O6 oxygen atoms in **I** and **II** and twofold disordered PEG400 ($HO–CH_2–CH_2–O–(CH_2–CH_2–O)_4–CH_2–CH_2–OH$) and two glycol molecules in **II**). During refinement, the sums of the occupation factors of each of these O6 atom pairs and the sums of major and minor I sites were fixed at 1.0, C–H hydrogen atoms were placed into calculated positions at C–H bond length of 0.97 Å and their parameters were varied according to the 'riding' model. To avoid overfitting of the models, 5% of the reflections were flagged for calculation of R_{free} before initiating the refinement.[28] Refinement statistics for crystal structures **I** and **II** are given in Table 1.

3. Results and discussion

Crystals of **I** have orthorhombic space group $C222_1$ with two CA26 in the asymmetric unit, formula 2 CA26·6 NH_4I_3·2 NH_4I·91.5 H_2O; crystals of **II** belong to the monoclinic space group $C2$ with half of the CA26 molecule in the asymmetric unit, formula $(CA26)_{0.5}$·$Ba_{0.5}$ I_3·$PEG400_{0.5}$·2 glycol·23.75 H_2O (glycol $C_2H_6O_2$ was present in PEG400 as impurity).

In both crystal structures, the macrocycle of CA26 is folded into a figure '8' as recently described,[20] Fig. 1. It is clearly divided into two halves with 13 glucoses each, G1–G13 and G14–G26, that are antiparallel and related by twofold axes passing right through the center of the molecule, i.e., a local pseudo-C_2 axis in **I** and a crystallographic C_2 axis in **II**. The two halves of CA26 are connected by band-flip motifs found thus far in all cycloamyloses with 10 and more glucoses in the macrocycles.[29] The characteristics of this motif are pairs of glucoses (G13–G14 and G26–G1) oriented *anti* and stabilized in this conformation by bifurcated (three-center) hydrogen bonds with $O3_n$–H as donor and $O5_{n+1}$ and $O6_{n+1}$ as acceptors. By contrast, all the other glucoses in the two halves are oriented *syn* typical for amylose and cyclodextrins so that $O3_n\cdots O2_{n+1}$ hydrogen bonds are formed. The two halves of each CA26

are folded into $1^2/_3$ turns long, left-handed V-amylose helices (formed by 10 glucoses each) and stabilized by intramolecular $O6_n\cdots O2_{n+6}$ or $O6_n\cdots O3_{n+6}$ hydrogen bonds between glucoses in adjacent turns, with C6–O6 in the preferred (+) *gauche* orientation within helical turns and the less preferred (−) *gauche* orientation in some of the glucoses near the end of the V-helices, respectively. The conformations of glucoses, inter-glucose torsion angles ϕ, ψ and hydrogen bonds between adjacent glucoses in CA26 are similar to those reported recently.[19,20]

In addition to the intramolecular hydrogen bonds, the folding of CA26 is stabilized by water molecules W1 to W4 which crosslink the helical segments (W1 and W2 are shown in Fig. 1; W3 and W4 are located 'behind' W1 and W2 and hidden by atoms of CA26). Since these water molecules were found in comparable positions in all CA26 structures determined thus far, they must be considered as essential structural motifs.

In **I**, the glucoses of the two CA26 molecules in the asymmetric unit are denoted as G1–G26 and G101–G126, respectively. The CA26 molecules are stacked such that the helical segments form $2 \times 1^2/_3$ turns long V-amylose pseudo-helices. They are stabilized by intermolecular hydrogen bonds that are direct O3(G1)···O3(G114) and O6···O6′ between glucoses G22–G25 and G113–G110 (Fig. 2(A)) but both direct and mediated by water O6···O_W···O6′/O5′ between glucoses G11–G13 and G123–G125 (Fig. 2(B)). The NH_4^+ cations in **I** could not be distinguished from water molecules and are consequently considered to be water.

The molecular arrangement is different for **II** as V-helices of adjacent CA26 interact with their O2/O3 sides, G1–G4 of one CA26 hydrogen bonding to G4′–G1′ of the adjacent one. Ba^{2+} is located at the interface (and right on the crystallographic C_2 axis), and coordinated by twofold disordered PEG400 and by two glycol molecules, Fig. 3. The coordination of Ba^{2+} with PEG400 is similar as previously described.[30]

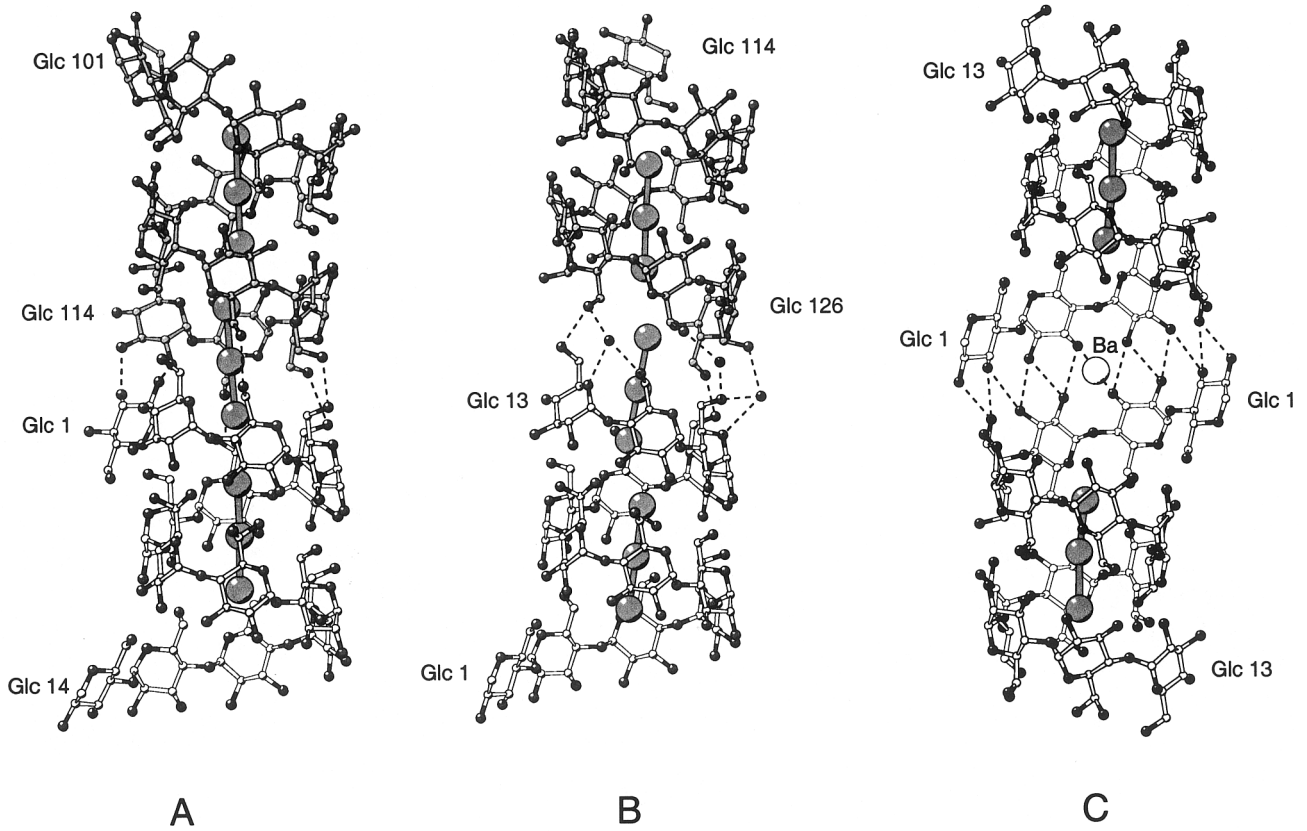

Fig. 2. Connectivity between adjacent CA26 molecules in **I** (A and B) and in **II** (C). In (A), two different CA26 are stacked and connected by direct O3···O3′ and O6···O6′ hydrogen bonds (dashed lines) to form a channel with $2 \times 1^2/_3$ turns V-helix. Oxygens dark grey, carbons white/grey, iodines large grey spheres, glucoses numbered G14 to G26 + G1 for the lower (white) CA26, and G101 to G113 + G114 for the upper (grey) CA26. (B). In the 'second' channel two adjacent CA26 are connected by direct O6···O6′ and by water-mediated hydrogen bonds O6···W···O6′/O5′ indicated by dashed lines. Note that the lowermost V-helical turns in (A) and (B) are comparable, i.e., glucoses G14 to G21 in (A) and G1 to G8 in (B), but the positions of the lowermost triiodides T3 (A) and T4 (B) are not, T3 being shifted 'upward' relative to T4 by about 1.5 Å. (C) Connectivity between adjacent CA26 molecules in **II**, hydrogen bonds between O2, O3 hydroxyl groups indicated by dashed lines. The crystallographic C_2 axis is perpendicular to the paper plane and passes right through Ba^{2+} (large sphere). Glucoses numbered G1 to G13, with oxygens in black and carbons in white, triiodides in grey, large spheres indicate iodine atoms I1, I2, I3.

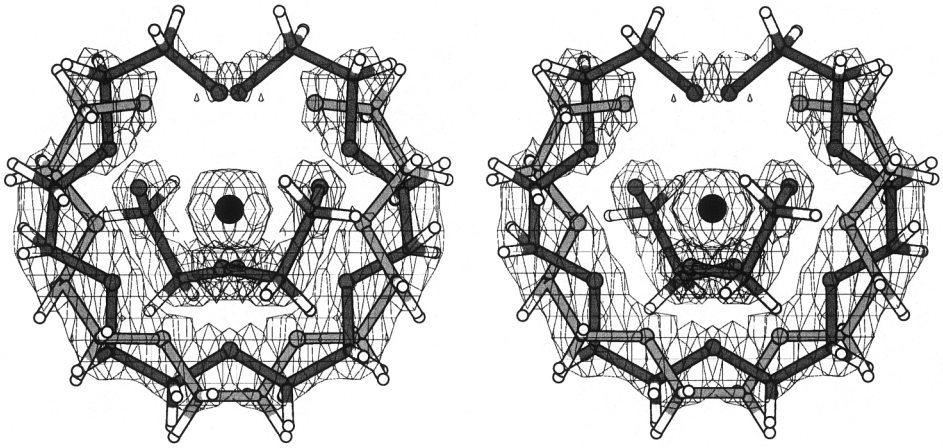

Fig. 3. Stereo view of the Ba^{2+} cation coordination in structure **II**. Electron density at the 1.0 σ level shown in thin lines and interpreted with Ba^{2+} (black sphere), two glycol molecules (center) and disordered PEG400 ($HO–CH_2–CH_2–O–(CH_2–CH_2–O)_4–CH_2–CH_2–OH$). O–C–C–O chains in grey, C–H bonds in white. The oxygen atoms coordinate Ba^{2+} at $Ba^{2+}\cdots O$ distances in the range 2.74–3.04 Å. A nearly identical geometrical arrangement has been found for Ba^{2+} tetra- and pentaethyleneglycol dimethylether thiocyanates.[30]

3.1. Packing of molecules in the unit cell

In crystals **II**, the packing of molecules is determined by the C_2 axis parallel to *b* that coincides with the inherent twofold rotation axis of CA26. These molecules are consequently arranged in the *a*, *c* plane. The $1^2/_3$ turns long V-helices are not stacked directly but separated by the $Ba^{2+}\cdots$PEG400 2 glycol complexes.

In **I**, the packing is much more complex with the triiodide (T) chains (T1–T2–T3 and T4–T5–T6) oriented nearly parallel to the *c*-axis (Fig. 4(a and b)). The two CA26 molecules in each asymmetric unit (indicated by red and blue colors in Fig. 4(a and b)) and the glucose units denoted G14 to G26 for one and G101 to G113 for the other CA26 harbour triiodide chains T1–T2–T3. The other chains T4–T5–T6 are located in the channels of CA26 from *different* asymmetric units and enclosed by glucose chains G1 to G13 from one and G114 to G126 from the other CA26. The two CA26 in an asymmetric unit are rotated by $\sim 60°$ about an axis formed by T1–T2–T3, yielding the complex zigzag pattern shown in Fig. 4(b).

3.2. Polyiodide chains

In both **I** and **II**, the V-amylose channels are filled by I_3^-. The channel in **I** is formed by two stacked CA26 ($2 \times 1^2/_3$) turns of V-helix and terminated at both sides by voids filled by water molecules. This contrasts the channel of **II** which is only one CA26 ($1^2/_3$) turns long and terminated by Ba^{2+} coordinated to PEG400 and 2 glycol, Fig. 3.

In **I**, each of the two symmetry-independent V-helix channels is occupied by two independent chains composed of three I_3^- (T1–T2–T3 and T4–T5–T6) that are twofold disordered and oriented along the crystallographic *c*-axis; for occupation factors see caption Fig. 5(A and B). One of the disordered chains has major occupation of the I_3^- units in the range 0.69–0.81 (T1–T2–T3 in one channel and T4–T5–T6 in the other channel, see Figs. 4 and 5(A and B)) and the other chain has minor occupation of 0.19–0.32. Since the I···I distances between these two major and minor occupied chains are in the range 0.74–1.62 Å, the chains exclude each other mutually, i.e., only one of the chains can be included in the V-channel at a time. Within the two chains, the I_3^- units are well defined, with I–I bond lengths in the range 2.81–3.00 Å (see Fig. 5(A and B)) and I1–I2–I3 angles in the range 174.7–179.2°. Between the I_3^- units, the I···I distances are much larger, 3.66–3.85 Å, but significantly shorter than the van der Waals separation, 4.3 Å.[31] The positional disorder of the I_3^- chains was already evident from diffuse streaks in the X-ray diffraction pattern of crystals of **I**, their separation of 3.1 Å reflecting the average distance along the polyiodide chains, similar as found in α-cyclodextrin-polyiodide and in amylose–iodine complexes.[16,5,6] In the channel of **II**, there is only one twofold disordered I_3^-, both sites with low occupation, 0.32 (major) and 0.11 (minor), Fig. 5(C).

The interactions between iodine atoms/ions and the V-helix channel (Table 2) are predominantly of type C5–H···I (32 contacts in **I** and 8 in **II** in the range 3.18–3.50 Å, comparing well with the van der Waals H···I distance of 3.35 Å). Although feasible from a geometrical point of view, there are much less C3–H···I contacts (2 in **I** and 3 in **II** in the range 3.35–3.50 Å) and an intermediate number of contacts for C6–H···I (11 in **I** and 5 in **II** in the range 3.32–3.57 Å). In addition, there are several O6···I interactions (with O6

in (+) *gauche* orientation, see Table 2) near the ends of the channels, 7 in **I** in the range 3.50–3.95 Å and 3 in **II** in the range 3.40–3.65 Å, close to the van der Waals O···I distance of 3.55 Å. There is no interaction <4.01 Å of the form O4···I, O2···I and O3···I as these oxygen atoms are further away from the central channel There is one exception found at the very end and in fact not part of a V-helix, G101 O2···I3 of T3, at 3.68 Å distance, Table 2.

3.3. Two I^- sites in I

Besides the triiodide chain filling the channels of the V-helices in **I**, there are two I^- sites, I7 and I8, Fig. 6. The former is located on the pseudo-C_2 axis and two-fold disordered with major (0.42) and minor (0.06) occupancy sites that are very close together (0.7 Å). The coordination of the major site is a distorted bipyramid with six H atoms forming a plane. They belong to two adjacent CA26 molecules, H1 of G110′ and H4 of G109′ to one CA26 and H1, H2 of G7 and G20 in the other CA26 (the pseudo-C_2 axis is located between G7 and G20 of the latter CA26) with H···I^- distances of 2.98–3.24 Å. The apical positions of the bipyramid are occupied by water molecules W63 and W149 at O···I^- distances of 3.45 and 3.58 Å, respectively. The other iodide, I8, is also only partially occupied (0.18) and located at the interface between two V-helices. It is sevenfold irregularly coordinated to O6 of G8 and O6 (disordered) of G9; O3 and H2 of G13 (at O···I^- distances in the range 3.26–3.47 Å and H···I^- at 3.39 Å), to H1 of G125′ (H···I^- at 3.00 Å) and to water molecules W32, W70 at 3.49 and 3.69 Å, respectively. A comparable albeit not identical coordination of I^- by α-cellobiose was recently reported.[32] Since in this latter study all O–H hydrogen atoms were located and all

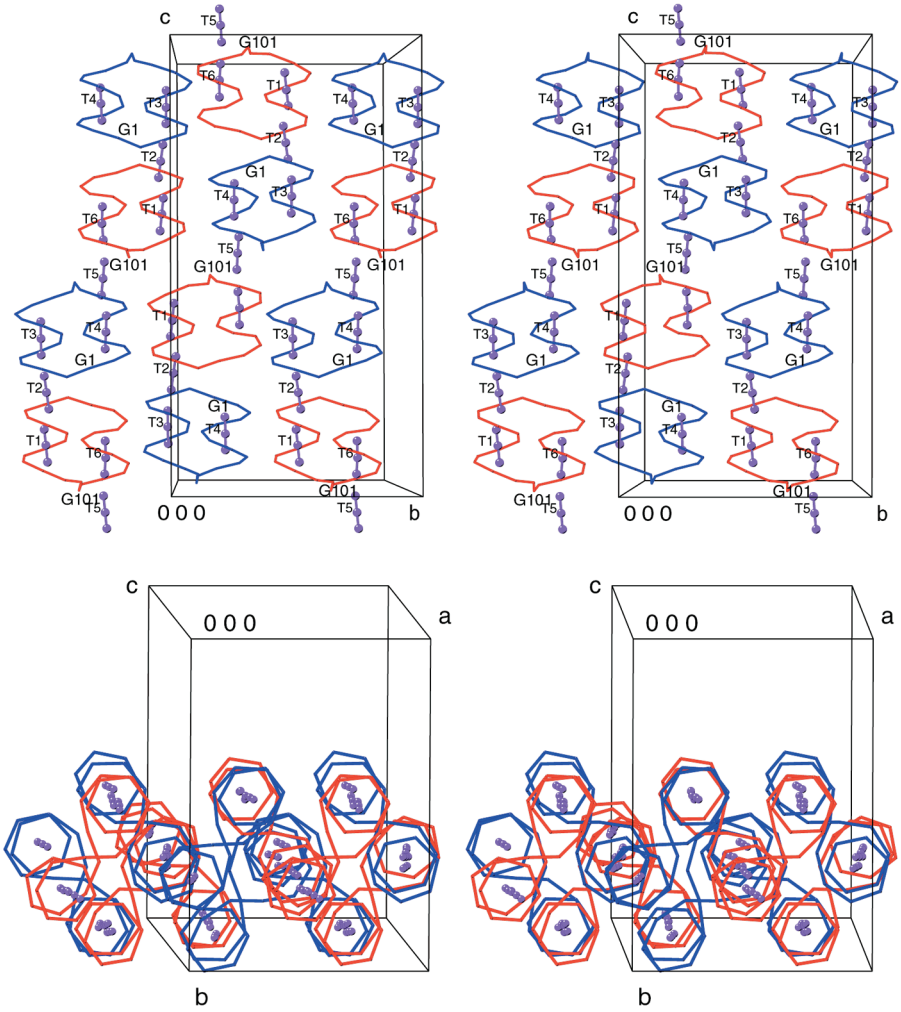

Fig. 4. Stereo views illustrating the packing of CA26 and triiodide molecules in structure **I**. (Top, **a**) View on the *b*,*c* plane. The unit cell contains 4 asymmetric units (a.u.), each harbouring two CA26 indicated in red and blue and denoted G1 and G101 at the positions of glucoses G1 and G101. Note that triiodide chain T1–T2–T3 is bound to two CA26 of the same a.u. whereas chain T4–T5–T6 is bound to two CA26 of different a.u. (Bottom, **b**) View on the *a*, *b* plane, same coloring as in (A). Note that the two CA26 in each a.u. are rotated by about 60° with respect to each other, with T1–T2–T3 and T4–T5–T6 acting as rotation axes.

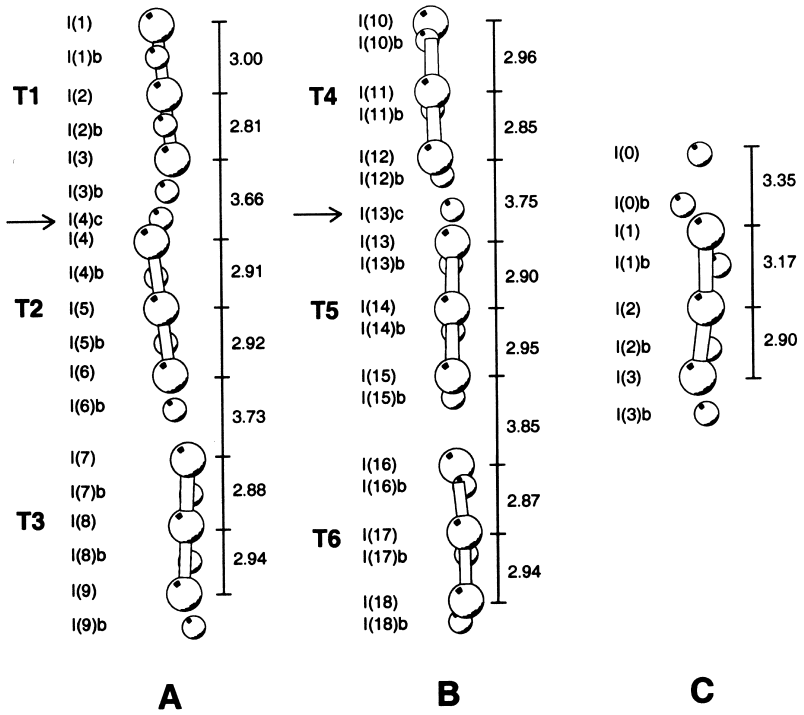

Fig. 5. Geometry of triiodide chains in **I** (A, B) and in **II** (C). Major occupancy sites (T1 0.69, T2 0.72, T3 0.68, T4 0.71, T5 0.80, T6 0.81) shown in ball-and-stick representation with large spheres and denoted I(1), I(2), I(3) etc., low occupancy sites (T1 0.31, T2 0.28, T3 0.32, T4 0.29, T5 0.20, T6 0.19) with small spheres and denoted I(1)b, I(2)b, I(3)b etc. Two extra sites I(4)c and I(13)c with occupancy of 0.20 and 0.28 are marked by horizontal arrows as they could not be attributed to I_3^-. Numbers at vertical bars to the right of the triiodide chains indicate I–I distances of the major occupancy I_3^- and between the I_3^- units.

O–H groups are engaged in coordination to I^- with their H atoms forming O–H···I^- interactions, we assume that in our study as well it is not the O–H oxygens that coordinate I^- but rather the O–H hydrogens that could, however, not be located.

3.4. Raman spectra

Model compounds of polyiodides provided an assignment of Raman spectra to different species: Raman bands at 190 cm^{-1} to I_2; strong bands between 100 and 120 cm^{-1} (ν_1) to linear I_3^-, and bands in the 130–155 cm^{-1} region (ν_3) to asymmetric I_3^-; bands at 75, 90 and 163 cm^{-1} to linear I_5^- and at 76, 112, 145 and 155 cm^{-1} to bent I_5^-.[9,10] A band at 104 cm^{-1} in the Raman spectrum of a model compound (trimesic acid·I_5^-) was initially assigned to I_5^-[10] but later suggested to be due to impurities of I_3^- because theoretical and far-infrared studies assigned the band near 110 cm^{-1} to I_3^- and not to I_5^-.[3,9]

Raman spectra taken from single crystals of **I** show bands at 107 and 141 cm^{-1} that are clearly consistent with the presence of I_3^- and provide conclusive evidence for the assignment of these bands to I_3^- (Fig. 7). When the crystals were dissolved in water, a strong I_3^- band comparable to that of the crystal spectrum was found at 110 cm^{-1}, however, different to the crystal spectrum two major bands were found at 150 and 168 cm^{-1} that indicate the presence of complicated vibrational states of the iodide species in solution (Fig. 7). The 150 cm^{-1} band points to the presence of I_3^- (ν_3 vibrations of asymmetric I_3^-) whereas the strong band at 168 cm^{-1} suggests the presence of another species. This might be a distorted I_3^- or linear I_5^-. Weaker bands at 227, 281, 334 cm^{-1} could be assigned to combinations of overtone frequencies of the major bands. The Raman spectrum of **II** dissolved in water (Fig. 7) has the same

Table 2
Polyiodide-oxygen contacts <4.0 Å of **I** and **II**

Res/Atom I	Res/Atom J	Distance IJ (Å)
T1 I1	102 O6	3.50
T2 I3	22 O6	3.64
T3 I1	19 O6	3.95
T3 I1	20 O6	3.61
T3 I2	19 O6	3.79
T5 I1	9 O6	3.85
T5 I3	101 O2	3.68
I1	7 O6	3.65
I2	5 O6	3.56
I3	3 O6	3.40

All O6 in (+) *gauche* orientation, most are disordered.

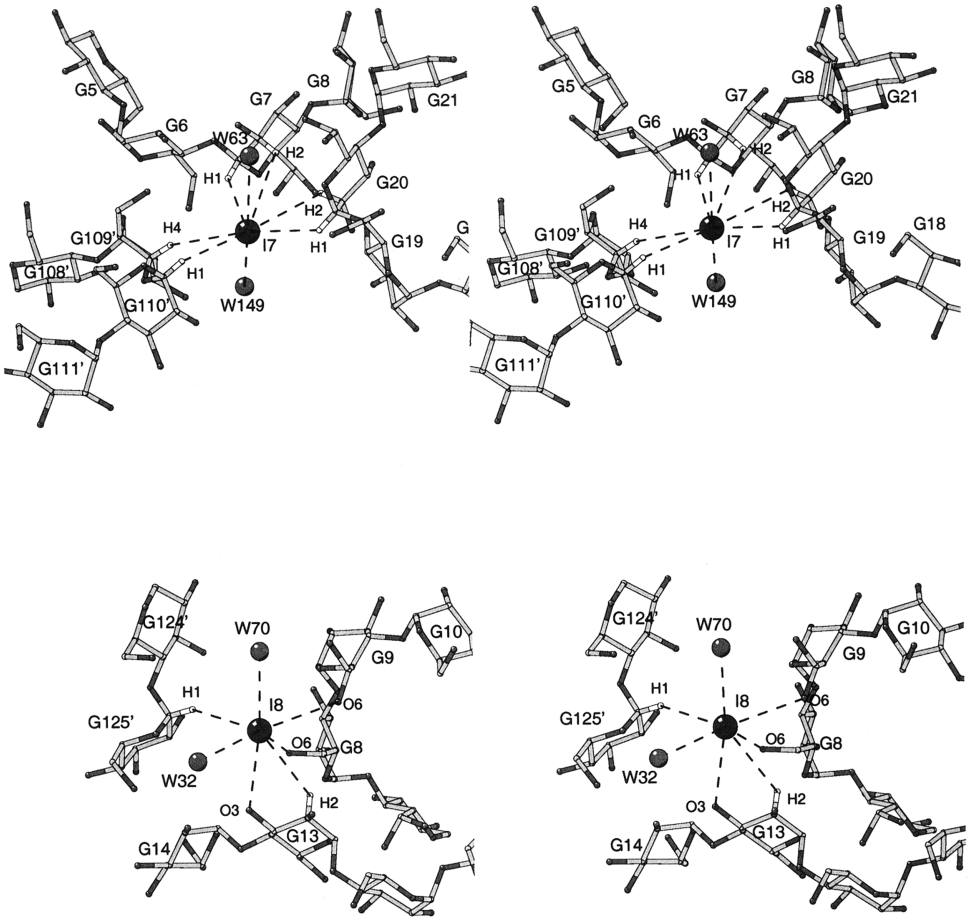

Fig. 6. Coordination of the two iodide anions I7 (Top) and I8 (Bottom) in crystals of **I**. In (Top), only the major occupancy site of I7 is shown. Coordinated H atoms and O–H groups are indicated by dashed lines and distances (Å) are given in the text.

spectral features as that of **I** dissolved in water, suggesting the same interpretation as given above.

Principal bands at 109 and 160 cm^{-1} have been observed in the Raman spectra of starch–iodine complexes.[3,7,10] The band at 109 cm^{-1} confirms the presence of I_3^- as main component in starch–iodine complexes, and the strong band at 160 cm^{-1} points to the presence of I_5^-, with I_3^- and I_5^- being key substructures in the polyiodide chain.[3] The two species function cooperatively and define the electronic excitations that are responsible for the deep blue color of the complexes.[3] The band near 110 cm^{-1} in the Raman spectra of starch–iodine and in complexes **I** and **II** supports the view that **I** and **II** represent good models for certain amylose iodine properties. The spectral features in the region around 160 cm^{-1}, however, clearly indicate differences between **I** and **II** in the crystal and in solution and between the solution properties of **I** and **II** and amylose–iodine.

3.5. Absorption spectra

Absorption spectra recorded with the NH_4I_3 and $Ba(I_3)_2$ solutions used for crystallization of **I** and **II** did not indicate the presence of molecular iodine, $\lambda_{max}(I_2) = 460$ nm, suggesting that the solutions contained only I_3^- and I^-. Absorption spectra taken from thin crystals of **I** and **II** and from aqueous solutions of these crystals showed bands at 287 and 368 nm (not shown), indicating the presence of I_3^- and I^-. These absorption maxima are consistent with the brown color of crystals of **I** and **II**. For amylose–iodine, the absorption maximum is in the range 566–572 nm depending on conditions and in agreement with the deep blue color of 'iodine's blue'. A similar deep blue/black color (with metallic luster) was reported[16] for the channel-type complexes formed by α-cyclodextrin and $LiI_3 \cdot I_2$ and $Cd(I_3)_2 \cdot I_2$, respectively, where the disordered $I_3^- \cdot I_2$ chains are of infinite lengths and not only limited to three or one I_3^- as in **I** and **II**, respectively.

3.6. Conclusions

This study describes the inclusion complexes of CA26 with NH_4I_3 (**I**) and $Ba(I_3)_2$ (**II**). In **I**, two CA26 molecules are stacked on top of each other, providing

channels with nearly $2 \times 1^2/_3 = 3^1/_3$ V-helical turns. These channels are filled by three I_3^-, the two 'outer' ones are located within the two CA26 channels, and the 'central' one occupies a position between the two stacked CA26 molecules. In **II**, the two channels are isolated, each one being occupied by one I_3^- similarly located as the 'outer' I_3^- in complex **I**. The existence of only I_3^- (and not I_2 or I_5^- or any higher polymorph) is also evident from Raman spectra taken from crystalline **I** and **II**.

These findings are in agreement with isothermal titration calorimetry (ITC)[33] which has shown that CA26 accommodates one I_3^- each in two identical sites with different binding constants $K_1 = 3.29(5) \times 10^3\ M^{-1}$ and $K_2 = 16.4(2) \times 10^3\ M^{-1}$, respectively. The difference in K_1 and K_2 indicates that the binding sites are not independent but influence each other, suggesting that slight molecular distortions occur upon binding of the first I_3^- to CA26 and are transmitted to the second channel, thereby modulating the binding of the second I_3^-. All studied CA from CA21 to CA32 show different binding constants (with maxima for CA24 ($K_1 \sim 2 \times 10^3\ M^{-1}$, $K_2 \sim 57 \times 10^3\ M^{-1}$) and CA31 ($K_1 \sim 5 \times 10^3\ M^{-1}$, $K_2 \sim 62 \times 10^3\ M^{-1}$). For all CA, ΔH and $-T\Delta S$ compensate for each other and show a maximum of 112.8 kJ mol^{-1} for CA26. This indicates that ΔG is relatively small (-20– -30 kJ mol^{-1} for all investigated CA21 to CA32), and similar values have been obtained for inclusion complex formation of the common α- and β-cyclodextrins.[33] These findings are probably associated with the release of structural water molecules from the interacting surfaces (I_3^- and channel-like cavities in CA26) and formation of hydrogen bonds in bulk water.[21]

The interactions between I_3^- and CA26 are mainly of the type C5–H···I and C6–H···I, with only few of type C3–H···O. There is no interaction with oxygen atoms O4, O5, O2–H and O3–H as they are more than 4.01 Å away from the iodine atoms except for O2 of G101 located at the end and outside the V-helix at O2···I of 3.68 Å. With O6, however, several contacts are formed, O6···I, within the range 3.50–3.95 Å and only if O6 is in the (+) *gauche* orientation and close to the end of the V-helix. These data indicate that the frequently proposed O4···I charge-transfer interactions cannot play a role in the amylose–iodine complex.

The color of the CA26·I_3^- complexes **I** and **II** is brown and not blue–black as found in amylose–iodine[5–7] and in the structurally studied complexes of α-cyclodextrin and $I_3^-\cdots I_2$ or I_5^-.[16] This could be due to the limited lengths of the T1–T2–T3 and T4–T5–T6 triiodide chains. Since, however, the triiodide chains are 'infinitely' long in the complex formed between *p*-nitrophenylmaltohexaose and I_3^- and the color of these crystals is also brown and not blue–black, it appears that polyiodide chains containing I_3^- and I_2 are required to produce the deep color characteristic for amylose–iodine.

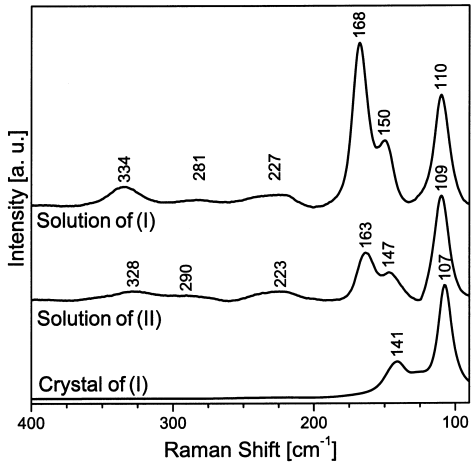

Fig. 7. Raman spectra of crystals of **I** (bottom) and of solutions (crystals dissolved in water) of **I** (top) and **II** (middle). The spectrum of a crystal of **I** was measured with excitation wavelength of 1064 nm using an RSF 100 FT-Raman spectrometer (Bruker, Germany). The spectra of solutions of **I** and **II** were measured with excitation at 514.5 nm using a T64000 Raman spectrometer (Jobin Yvon, France) in triple additive mode. All spectra were taken at room temperature (about 23 °C).

4. Supplementary material

The atomic parameters have been deposited with the Cambridge Crystallographic Data Centre, CCDC Nos. 177578 and 177894 for compounds **I** and **II**. Copies of this information may be obtained free of charge from The Director, CCDC, 12 Union Road, Cambridge, CB2 1EZ, UK (Fax: +44-1223-336-033; e-mail: deposit@ccdc.cam.ac.uk or www: http://www.ccdc.cam.ac.uk).

Acknowledgements

The described studies were financially supported by Deutsche Forschungsgemeinschaft and Fonds der Chemischen Industrie. We are grateful to Dr Takeshi Takaha, Ezaka Glico Co. Ltd., Osaka 555, Japan for supplies of purified CA26 and to HASYLAB/DESY for synchrotron X-ray beam time. Dr W.-D. Hunnius, Free University Berlin, helped with the Raman spectrum of **I**.

References

1. Colin, J. J.; Gauthier de Claubry, H. *Ann. Chim. Ser.* **1814**, *1* (90), 87–100.

2. Tomasik, P.; Schilling, C. H. *Adv. Carbohydr. Chem. Biochem.* **1998**, *53*, 263–343.
3. (a) Yu, X.; Houtman, C.; Atalla, R. H. *Carbohydr. Res.* **1996**, *292*, 129–141;
(b) Handa, T.; Yajima, H. *Biopolymers* **1980**, *19*, 1723–1741.
4. Calabrese, V. T.; Kahn, A. *J. Phys. Chem.* **2000**, *104*, 1287–1292.
5. Rundle, R. E. *J. Am. Chem. Soc.* **1947**, *69*, 1769–1772.
6. Bluhm, T. L.; Zugenmaier, P. *Carbohydr. Res.* **1981**, *89*, 1–10.
7. (a) Pfannemueller, B.; Ziegast, G. *Starch/Stärke* **1983**, *35*, 7–11;
(b) Ziegast, G.; Pfannemueller, B.; *Int. J. Biol. Macromol.* **1982**, 4, 9–17 and 419–424.
8. Latte, B.; Kienast, A.; Bruhn, C.; Loidl, A.; Homborg, H. *J. Phorphyrins Phthalocyanin* **1997**, *1*, 267–273.
9. Nour, E. M.; Chen, L. H.; Laane, J. *J. Phys. Chem.* **1986**, *90*, 2841–2846.
10. Teitelbaum, R. C.; Ruby, S. L.; Marks, T. J. *J. Am. Chem. Soc.* **1980**, *102*, 3322–3328.
11. Minick, M.; Fotta, K.; Khan, A. *Biopolymers* **1991**, *31*, 57–63.
12. Konishi, T.; Tanaka, W.; Kawai, T.; Fujikawa, T. *J. Synchrotron Rad.* **2001**, *8*, 737–739.
13. Lin, Z.; Hall, M. B. *Polyhedron* **1993**, *12*, 1499–1502.
14. Sharp, S. B.; Gallene, G. I. *J. Phys. Chem., Sect. A* **1997**, *101*, 2192–2197.
15. Hinrichs, W.; Büttner, G.; Steifa, M.; Betzel, C.; Zabel, V.; Pfannemüller, B.; Saenger, W. *Science* **1987**, *238*, 205–208.
16. (a) Noltemeyer, M.; Saenger, W. *Nature* **1976**, *259*, 629–632;
(b) Noltemeyer, M.; Saenger, W. *J. Am. Chem. Soc.* **1980**, *102*, 2710–2722.
17. Takaha, T.; Yanase, M.; Takata, H.; Okada, S.; Smith, S. M. *J. Biol. Chem.* **1996**, *271*, 2902–2908.
18. Terada, Y.; Yanase, M.; Takata, H.; Takaha, T.; Okada, S. *J. Biol. Chem.* **1997**, *272*, 15729–15733.
19. Gessler, K.; Usón, I.; Takaha, T.; Krauß, N.; Smith, S. M.; Okada, S.; Sheldrick, G. M.; Saenger, W. *Proc. Natl. Acad. Sci.* **1999**, *96*, 4246–4251.
20. Nimz, O.; Geßler, K.; Usón, I.; Saenger, W. *Carbohydr. Res.* **2001**, *336*, 141–153.
21. Kitamura, S.; Nakatani, K.; Takaha, T.; Okada, S. *Macromolecular Rapid Commun.* **1999**, *20*, 612–615.
22. Otwinowski, Z.; Minor, W. *Methods Enzymol.* **1996**, *276*, 307–326.
23. (a) Sheldrick, G. M.; Hauptman, H. A.; Weeks, C. M.; Miller, R.; Usón, I. Ab initio phasing. In *International Tables for Crystallography*; Arnold, E.; Rossmann, M., Eds.; Kluwer Academic Publ: Dordrecht, 2001; Vol. F, pp 333–351;
(b) Usón, I.; Sheldrick, G. M. *Curr. Opin. Struct. Biol.* **1999**, *9*, 643–648.
24. Karle, J. *Acta Crystallgr., Sect. B* **1968**, *27*, 182–186.
25. Fujinaga, M.; Read, R. J. *J. Appl. Cryst.* **1987**, *20*, 517–521.
26. Sheldrick, G. M.; Gould, R. O. *Acta Crystallogr., Sect. B* **1995**, *51*, 423–431.
27. Sheldrick, G. M.; Schneider, T. R. *Methods Enzymol.* **1997**, *277*, 319–343.
28. Brünger, A. T. *Nature (London)* **1992**, *355*, 472–475.
29. Jacob, J.; Geßler, K.; Hoffmann, D.; Sanbe, H.; Koizumi, K.; Smith, S. M.; Takaha, T.; Saenger, W. *Angew. Chem., Int. Ed. Engl.* **1998**, *37*, 605–609.
30. Wie, Y.Y.; Tinant, B.; DeClercq, J.-P.; van Meerssche, M.; Dale, J.; *Acta Crystallogr.* 1987, C43, 1076–1080 and 1270–1274.
31. ; Weast, R. C., Ed. *Handbook of Chemistry and Physics*, 57 ed.; CRC Press: Cleveland, OH (USA), 1977; p D-178.
32. Peralta-Inga, Z.; Johnson, G. P.; Dowd, M. K.; Rendleman, J. A.; Stevens, E. D.; French, A. D. *Carbohydr. Res.* **2002**, *337*, 851–861.
33. v. Rekharsky, M.; Inoue, Y.; *Chem. Rev.* 1998, 98, 1875–1917.